J. Phys. Chem. A **2003,** *107,* 2855−2859

Oxidative Degradation of Small Cationic Vanadium Clusters by Molecular Oxygen: On the Way from V_n^+ ($n = 2-5$) to VO_m^+ ($m = 1, 2$)

Marianne Engeser, Thomas Weiske, Detlef Schröder,* and Helmut Schwarz*

Institut für Chemie der Technischen Universität Berlin, Strasse des 17. Juni 135, D-10623 Berlin, Germany

Received: October 10, 2002; In Final Form: January 16, 2003

Ion-cyclotron resonance mass-spectrometric experiments are used to examine the reactions of small cationic vanadium clusters V_n^+ and vanadium-oxide clusters $V_nO_m^+$ ($n \leq 5$, $m \leq 3$) with molecular oxygen. Most of these reactions are very fast ($k \geq 3 \times 10^{-10}$ cm^3 molecule^{-1} s^{-1}) and strongly exothermic. Oxidative degradation of the clusters (decreasing n) is generally more favored than oxygen-transfer resulting in $V_nO_m^+$ cations (constant n). Consequently, the mononuclear oxide ions VO^+ and VO_2^+ evolve as the major final products at the end of a reaction cascade. For V_2^+ and V_3^+, the complete network of elementary steps is explored by MS/MS experiments. Furthermore, some thermochemical brackets are derived, e.g., for the enthalpies of formation of the ions $V_2O_m^+$ ($m = 1-3$): 920 kJ/mol $\leq \Delta_fH$ (V_2O^+) $\leq$ 1130 kJ/mol; 670 kJ/mol $\leq \Delta_fH$ ($V_2O_2^+$) $\leq$ 880 kJ/mol, and 420 kJ/mol $\leq \Delta_fH$ ($V_2O_3^+$) $\leq$ 630 kJ/mol.

Introduction

Vanadium-oxide compounds are widely used in industrial processes. They serve as support for heterogeneous catalysts, but also as active catalysts on their own, i.e., in the production of SO_3 from SO_2, of propene from propane, and of maleic anhydride from butane.[1] Nevertheless, the physical and chemical origin of their activity is still not clear and therefore widely debated.[2] If oxidation occurs via a Mars-Van-Krevelen mechanism,[3] the oxidized substrate contains only oxygen atoms taken from the surface, which in turn is reoxidized by molecular oxygen in a separate, second step. Transition-metal clusters as well as their oxides can be regarded as suitable model systems to investigate the elementary steps involved in industrial catalysis because clusters of different sizes and compositions often form the surface structure of heterogeneous catalysts. Therefore, the reactions of vanadium- and vanadium-oxide clusters with molecular oxygen should provide valuable new insight. A simple way to examine these systems is to study gas-phase reactions of cluster ions. The means of mass spectrometry ensure that the reaction conditions are well-defined and controlled in an easy and reproducible way without interference of surface defects, solvent effects, impurities, temperature gradients, etc. Because of favorable MS/MS capabilities, the Fourier transform ion-cyclotron resonance (FT-ICR) technique is especially suited for the investigation of multiply branched consecutive reactions.[4] Moreover, the high mass-resolving power allows unambiguous assignments of the ions' elemental compositions.

Gas-phase vanadium-oxide clusters have previously been examined theoretically[5−7] as well as experimentally.[8−14] The oxidation of neutral vanadium clusters V_n of medium size ($n = 10-60$) with O_2 has been described by Holmgren and Rosén,[13] whereas Xu et al. have studied the reaction of small cationic vanadium clusters V_n^+ ($n = 2-17$) with molecular oxygen using a guided ion beam apparatus.[14] In extension to our earlier study of the oxygenation of atomic V^+ in the presence of O_2,[8] the reactions of small cationic clusters V_n^+ with O_2 are reported here. The aim of our work was to explore further the kinetics of these reactions, to study the reactivity of the oxides formed in the initial step, and to compare the results obtained with our new cluster source with the thermochemical data provided by previous studies.

Experimental Section

The reactions reported herein have been investigated using a Spectrospin CMS 47X FT-ICR mass spectrometer[15] equipped with a newly built external cluster-ion source of the Smalley-type[16] developed by the group of Niedner-Schatteburg.[17] This new source is situated in a vacuum chamber consisting of a standard DN 160 clamp flange 6-way cross pumped by a magnetically shielded turbomolecular pump (TPH 330, Pfeiffer Vacuum GmbH). With the aid of an adaptor flange, the 6-way cross fits to the housing of the previously mounted ion source. This housing now contains some static transfer ion-optical elements. For ease of use, we have replaced the originally built-in piezo valve by a pulsed solenoid valve (Parker Hannifin Corp., General Valve Division, model 91-74-900, DC 20 V operation voltage, 0.8 mm diameter outlet orifice) controlled by a commercially available solenoid valve controller (Parker Hannifin Corp., General Valve Division, model Iota One). Solenoid valve, laser, and ICR-cell gate pulses and delays have been manually controlled by a four-channel digital pulse/delay generator (S. M. V. Systemelektronik GmbH, model PDG 204) that is triggered by the Aspect 3000 computer of the CMS 47X.

A typical experiment starts with a helium gas pulse (Messer Griesheim GmbH, 99.999% purity, varied up to 40 bar) in the direction of the ion-beam axis, which is parallel to the magnetic field within the ICR-magnet. A laser shot from a pulsed Nd:YAG laser (Spectron Systems, pulse length 6−8 ns, maximum output energy 170 mJ per pulse, 5 Hz repetition rate) operating at its fundamental wavelength (1064 nm) is focused onto the surface of a rotating vanadium disk. The hot metal plasma is cooled by the expanding helium gas and travels through a metal tube (2 mm inner diameter, 45 mm length) in which clustering takes place. Behind the flow tube and a free gap of ap-

---

* To whom correspondence should be addressed. Phone: +49 30 314 23483. Fax: +49 30 314 21102. E-mail: df@www.chem.tu-berlin.de.

10.1021/jp0222088 CCC: $25.00

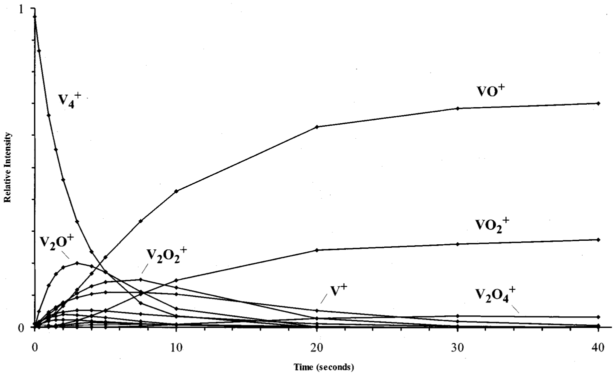

Figure 1. Intensities of ions detected during the reaction of V_4^+ with O_2 as a function of time; $p(O_2) = 1.2 \times 10^{-8}$ mbar.

proximately 20 mm in length, the molecular beam is restricted by a skimmer (Beam Dynamics Inc., model 2, 0.78 mm orifice diameter, hyperbolically shaped). Afterward, it passes a series of potentials and ion lenses[15] to guide the remaining charged components of the molecular beam into the ICR cell, which is positioned in the bore of a 7.05 T superconducting magnet. The ion of interest is isolated by the FERETS technique,[18] and the reaction with molecular oxygen (Linde AG, 99.995% purity) is monitored at a constant reaction pressure of 1.2×10^{-8} mbar. The experimental second-order rate constants are evaluated assuming the pseudo-first-order kinetic approximation after calibration of the measured pressures and acknowledgment of the ion gauge sensitivities; the error of the absolute rate constants is assumed to be ±30%. Using helium pressures in the range of 3−6 bar and a valve opening time of about 150 μs, we were able to detect cluster distributions V_n^+ up to the size of $n = 10$.

It is important to keep the helium cooling-gas as pure as possible to obtain stable, reproducible, and long lasting cluster-ion beams.[19] Connecting tubes, fittings, and valves between the helium gas bottle and the pulsed valve should be made of stainless steel only. Any rubber seals, like the O-rings widely used in quick connectors, must be avoided. The transfer line was purged by passing helium through a flexible hose made of stainless steel which was heated at 200 °C (Horst Laborgeräte GmbH, 1m length, maximum temperature 250 °C). It is located directly behind the pressure regulator of the helium bottle. The hot helium which is guided by a coaxial rod up to the pulsed valve heats the rest of the transfer line and removes any volatile impurity from inside by its flow into a liquid nitrogen trapped rotary pump. During measurements, the transfer line is set to room temperature. Using this procedure, we obtained spectra of pure V_n^+-cluster distributions without traces of vanadium oxides.

To investigate the secondary reactions, the clusters have been allowed to react with dioxygen for 3−5 s before the desired oxide was mass-selected and further investigated as described above.

Results

Our interest is focused on the reactivities and properties of relatively small vanadium-cluster ions V_n^+ ($n \leq 5$), because only limited cluster sizes may allow to unravel the various reaction cascades and to elucidate mechanistic details.

The consecutive oxidation of V_4^+ in the presence of O_2 (Figure 1) is a typical case which may serve to illustrate the overall picture of the reactions studied here. During the first few seconds, many different ions are observed, which are either formed directly or stem from secondary reactions. At longer reaction times, however, the spectra are dominated by two peaks only, which correspond to the mononuclear species VO^+ and VO_2^+. Under ICR-conditions, these ions do not react any further with O_2.[8] Other ions containing more than one vanadium atom (mainly $V_2O_4^+$) are detected with intensities of less than 2%.

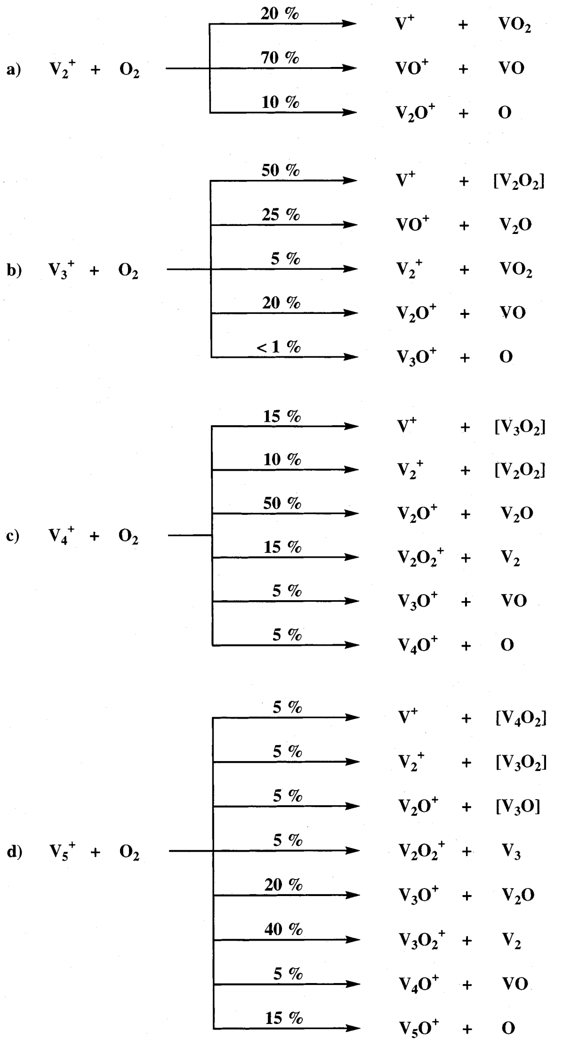

Figure 2. Primary branching ratios for the reactions of V_n^+ ($n = 2-5$) with O_2. The nature of the molecules given in brackets is not known; for example, $[V_2O_2]$ could either be intact divanadium dioxide V_2O_2 or two molecules of VO.

First, we concentrate on the initial step of these reaction cascades and analyze the primary branching ratios. The reaction of atomic V^+ with O_2 has already been described in detail[8] and under our experimental conditions exclusively leads to VO^+. Oxidation of the smallest cluster V_2^+ yields two major products (Figure 2), namely, VO^+ and V^+. In both cases, one vanadium atom is lost from the cluster to form neutral vanadium oxides. Only 10% of the molecules keep both metal atoms. Similarly, the main product in the oxidation of V_3^+ by O_2 is mononuclear V^+ concomitant with loss of the putative neutral V_2O_2. The monoxides VO^+ and V_2O^+ are both formed in comparable yields, whereas small amounts of two further products (V_2^+ and V_3O^+) are detected. The branching ratio of this reaction together with the more complicated ones of V_4^+ and V_5^+ are also shown in Figure 2 and the corresponding rate constants are summarized in Table 1. Note that due to the rapid growth of the VO^+ signal in Figure 1, the description of VO^+ as a secondary product in V_4^+ oxidation is not unambiguous, it could also be produced directly from V_4^+ in a slow primary reaction. However, as double-resonance experiments would not lead to any clear result

TABLE 1: Experimental Second-Order Rate Constants *k* and Reaction Efficiencies ϕ for the Oxidation of Small Vanadium Clusters with O_2

	V^+	V_2^+	V_3^+	V_4^+	V_5^+
k^a	2.7 [b]	2.5	5.9	7.5	11.1
ϕ	40% [b]	40%	100%	140%	200%

[a] Given in 10^{-10} cm^3 molecule^{-1} s^{-1}. The error is assumed to be ±30%. [b] Taken from ref 8.

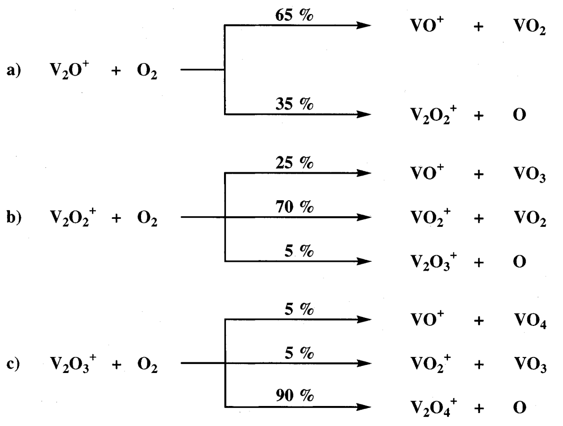

Figure 3. Primary branching ratios for the reactions of $V_2O_m^+$ ($m = 1-3$) with O_2.

(all intermediates give VO^+ in further reactions), this decision cannot be made here.

To obtain more decisive information about the subsequent reactions, we carried out MS/MS experiments. To this end, the ions formed in the first step are mass selected and their reactivity against O_2 is monitored separately. In this manner, it is possible to follow the whole reaction network step by step. Figures 3 and 4 show the primary reactions of $V_2O_m^+$ and $V_3O_m^+$ ($m = 1-3$) with molecular oxygen. Further, the $V_2O_4^+$ signal was too weak for MS/MS experiments, and we did not pursue toward $V_nO_m^+$ clusters with $n > 3$.

Discussion

All pathways for which the respective thermochemical data is known (Table 2 and last column of Table 3) are predicted to be strongly exothermic. Only the formation of V_2O^+ from V_2^+ is thermoneutral, a fact which is in accordance with the low percentage of this pathway in the branching ratio of V_2^+. As the oxidation of the pure metal clusters has already been studied in detail by guided ion-beam (GIB) experiments,[14] we extrapolated the reported cross sections to thermal energy to calculate primary branching ratios which can be compared directly to our ICR data. For V_2^+ and V_3^+, the numbers coincide within error bars, indicating very good agreement of the two different instrumental techniques. However, some notable deviations are found for the reactions of V_4^+ and V_5^+ with O_2. In these cases, we observe significant amounts of V^+ and V_2^+ as primary reaction products, which were not mentioned in ref 14.[20] Further, in the reaction of V_5^+ with O_2, the ion V_5O^+ is not detected at lowest energies in the GIB experiments, even though the reaction is predicted to be exothermic by 49 kcal/mol. Nevertheless, it is observed in our experiment with an appreciable yield.

A summary of all primary branching ratios for ions involved in the V_2^+/O_2 system provides the entire network of elementary steps for the oxidation of cationic divanadium with molecular oxygen. Based on this reaction cascade shown in Figure 5, the time dependencies of the ion signals in the V_2^+/O_2 system can be modeled reasonably well. Two aspects concerning the reactivity of $V_2O_3^+$ have to be pointed out in particular. First, $V_2O_3^+$ is the only intermediate in this system for which fragmentation in mononuclear ions does not prevail. Second, some small amounts of VO^+ are detected indicating the formation of neutral VO_4. This molecule is most probably an adduct of molecular oxygen and VO_2.[5a, 9c]

In the V_3^+/O_2 system, more than 99% of all V_3^+ ions lose one or more vanadium atoms in the initial reaction with O_2. Hence, the secondary reactions of the ions formed comprise those already discussed above for the V_2^+/O_2 system. The addition of an oxygen atom to the trivanadium oxide-clusters $V_3O_m^+$ ($m = 1-3$) again is disfavored compared to the various degradations to smaller clusters. Nevertheless, oxygen-atom transfer without fragmentation is one of the major routes for the oxidation of $V_3O_2^+$ resulting in $V_3O_3^+$.

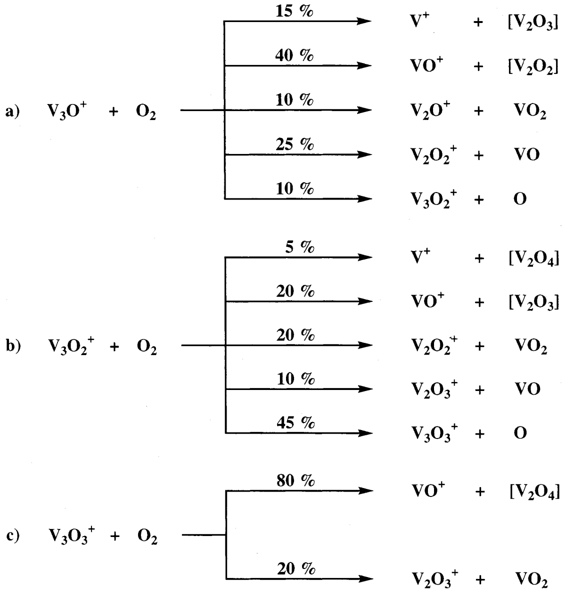

Figure 4. Primary branching ratios for the reactions of $V_3O_m^+$ ($m = 1-3$) with O_2. The nature of the molecules given in brackets is not known; for example, $[V_2O_2]$ could either be intact divanadium dioxide V_2O_2 or two molecules of VO.

TABLE 2: Relevant Enthalpies of Formation Δ_fH and Required Bond Dissociation Energies D_0, Electron Affinities EA, and Ionization Energies IE (all in eV) Taken from the Literature[26]

	Δ_fH (in kJ/mol)	calculated from	ref
V	515.5		a
V^+	1166	IE(V) = 6.746 ± 0.002	b
O	249.2		a
V_2	765	D_0(V−V) = 2.753 ± 0.001	c
V_2^+	1378	D_0(V^+−V) = 3.143 ± 0.003	c
V_3	1144 ± 10	D_0(V_2−V) = 1.42 ± 0.1	c
V_3^+	1675 ± 9	D_0(V_2^+-V) = 2.27 ± 0.09	c
V_4^+	1849 ± 12	D_0(V_3^+-V) = 3.53 ± 0.08	c
V_5^+	2052 ± 20	D_0(V_4^+-V) = 3.24 ± 0.17	c
VO	144 ± 19	D_0(V−O) = 6.44 ± 0.2	d
VO^+	842 ± 19	IE(VO) = 7.2386	e
VO_2	−232.6		a
VO_2^+	752 ± 40	D_0(OV^+−O) = 3.51 ± 0.36	f
VO_3	−283 ± 31	EA(VO_2) = 2.03 ± 0.01	g
		D_0(O_2V^--O) = 5.43 ± 0.31	f
		EA(VO_3) = 4.36 ± 0.05	g

[a] Chase, M. W., Jr. *NIST-JANAF Thermochemical Tables, Fourth Edition*, *J. Phys. Chem. Ref. Data* **1998**, *9*, 1−1951. [b] Reference 24. [c] Su, C. X.; Hales, D. A.; Armentrout, P. B. *J. Chem. Phys.* **1993**, *99*, 6616. [d] Pedley, J. B.; Marshall, E. M. *J. Phys. Chem. Ref. Data* **1983**, *12*, 967. [e] Harrington, J.; Weisshaar, J. C. *J. Chem. Phys.* **1992**, *97*, 2809. [f] Reference 10f. [g] Reference 9e.

TABLE 3: Brackets for Enthalpies of Formation $\Delta_f H$ and Bond Dissociation Energies $D_0(V_n^+ - mO)$ Derived by Thermochemical analysis of the Observed Reaction Pathways and Bond Dissociation Energies Given in Reference 14 for Comparison[26]

$V_nO_m^+$	reaction sequence used for calculation	$\Delta_f H$ in kJ/mol		$D_0(V_n^+ - mO)$ in eV		$D_0(V_n^+ - mO)$ in eV taken from ref. 14
		min	max	min	max	
V_2O^+	$V_2^+ \rightarrow\rightarrow VO^+$	967 ± 51	1129	5.16	6.8 ± 0.5	5.1 ± 0.3
$V_2O_2^+$	$V_2O^+ \rightarrow\rightarrow V_2O_3^+$	718 ± 51	880	10.32	12.0 ± 0.5	13.00 ± 0.41
$V_2O_3^+$	$V_2^+ \rightarrow\rightarrow VO^+$	469 ± 51	630	15.50	17.2 ± 0.5	
$V_2O_4^+$	$V_2O_3^+ \rightarrow$		381	20.66		
V_3O^+	$V_3^+ \rightarrow\rightarrow V_3O_2^+$	862 ± 54	1426 ± 9	5.16	11.0 ± 0.6	7.3 ± 0.3
$V_3O_2^+$	$V_3O^+ \rightarrow\rightarrow V_2O_3^+$	613 ± 54	1177 ± 9	10.32	16.2 ± 0.6	13.79 ± 0.41
$V_3O_3^+$	$V_3O_2^+ \rightarrow\rightarrow V_2O_3^+$	236 ± 51	927 ± 9	15.50	22.7 ± 0.5	
V_4O^+	$V_4^+ \rightarrow$		1600 ± 12	5.16		7.5 ± 0.3
V_5O^+	$V_5^+ \rightarrow$		1803 ± 20	5.16		7.3 ± 0.4

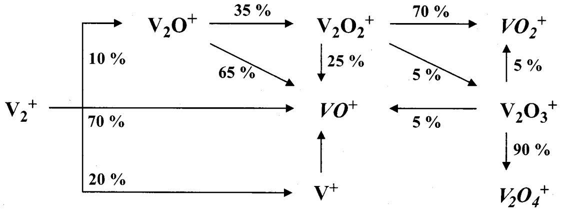

Figure 5. Complete reaction network for the oxidation of V_2^+ by O_2. Final products are printed in italics.

Next, let us address the rates of the various oxidation reactions. Usually, gas-phase rate constants are compared with gas-kinetic collision rates[21] to yield a measure of reaction efficiency. However, the efficiencies of several reactions reported here exceed 100%, and the deviation correlates with ion size (Table 1). A key assumption in the calculation of collision rates is that the reactions can be described as the interaction of a point charge with a polarizable neutral. Obviously, this may not be appropriate anymore for larger cluster ions. For example, the calculation of collision rates for clusters with more than 10 vanadium atoms has been performed using a hard-sphere model.[13]

Almost all reactions described here include both possible channels of charge distribution among the fragments. An analysis of the relative intensities of the possible charge distributions in the various pathways observed should provide some information about the ionization energies (IE) of the molecules involved.[22] For example, oxidation of V_4^+ with O_2 yields $V_2^+ + V_2O_2$ and $V_2O_2^+ + V_2$ in similar amounts, thus implying $IE(V_2O_2) \approx IE(V_2) = 6.36$ eV[23]. On the other hand, V_3^+ oxidation results in $V^+ + V_2O_2$ only, whereas no $V_2O_2^+$ is observed in this case. The conclusion of $IE(V_2O_2) \gg IE(V) = 6.75$ eV[23] contradicts the one drawn before. As electron-transfer reactions are usually assumed to proceed barrierless and therefore are a good means for evaluations of this kind, the key to understand this contradiction is the nature of the neutral products. Specifically, it is not sure that V_2O_2 is generated as an intact molecule, because even formation of two molecules of VO is still exothermic in these reactions. In addition, the production of two rather than one neutral molecule is favored entropically. Consequently, variable mixtures of different neutrals may evolve which surely cannot be compared in the way done above. Therefore, it is impossible to extract relative ionization energies from most of our data. Yet, a few conclusions can still be drawn.

VO_3 is always split off as a neutral. The same holds true for VO_2, except for the reactions $V_2O_2^+ + O_2 \rightarrow VO_2^+ + VO_2$ and $V_2O_3^+ + O_2 \rightarrow VO_2^+ + VO_3$. Thus, even though VO_2^+ is one of the major final products, it is not formed directly from pure metal clusters because of the large ionization energy of VO_2 (9.5 eV[25]). The occurrence of the reaction $V_2O_3^+ + O_2 \rightarrow VO_2^+ + VO_3$ without formation of the corresponding alternative pair VO_3^+/VO_2 is an experimental proof of $IE(VO_3) > IE(VO_2)$. Neutral VO_3 is a stable vanadium trioxide with a radical center on oxygen, whereas the cation VO_3^+ corresponds to a VO^+-O_2 complex.[5a] Our data fully agree with the rough picture of relative ionization energies extracted from experimental data given in ref 10d and the calculated ones given in ref 5a, according to which the ionization energy decreases with increasing cluster size and increases with increasing oxygen content.

The network of subsequent reactions reported here can be used for a rough bracketing of the enthalpies of formation for some of the intermediate ions, because only exothermic or thermoneutral reactions can be observed in an ICR experiment. For this thermochemical analysis, we use the auxiliary data given in Table 2. Deliberately, the data published in ref 14 is left out in order to compare the thermochemical results of the two experimental series independently. The enthalpies of formation deduced from our data are summarized in Table 3. The procedure is demonstrated for $\Delta_f H$ ($V_2O_2^+$). Of the various reactions in which $V_2O_2^+$ is formed or consumed, the narrowest brackets are obtained from the sequence $V_2O^+ \rightarrow V_2O_2^+ \rightarrow V_2O_3^+$. To this end, a lower limit for $\Delta_f H$ (V_2O^+) and an upper limit for $\Delta_f H$ ($V_2O_3^+$) are needed, which are derived from the following reactions:

$$V_2^+ + O_2 \rightarrow V_2O^+ + O \qquad \Delta_f H(V_2O^+) \leq 1129 \text{ kJ/mol}$$

$$V_2O_3^+ + O_2 \rightarrow VO_2^+ + VO_3$$
$$\Delta_f H(V_2O_3^+) \geq 469 \pm 51 \text{ kJ/mol}$$

Together with $\Delta_f H(O) = 249$ kJ/mol this leads to 718 ± 51 kJ/mol $\leq \Delta_f H(V_2O_2^+) \leq 880$ kJ/mol as given in Table 3.

All brackets reported here are quite large. The reason is the high oxophilicity of vanadium in lower oxidation states, which renders most reactions to be rather exothermic. Nevertheless, the brackets for the divanadium oxides $V_2O_m^+$ ($m = 1-3$) “only” span about 2 eV. Moreover, no experimental thermochemical data at all has been published so far for $V_nO_m^+$ ($n > 1$, $m > 2$). For an easy comparison, the GIB data from ref 14 is also included in Table 3. Most of the reported energies lie well inside our boundaries. The lower limit for the bond energy of V_2O^+ coincides with the reported value, this is another way to express that its formation is calculated to be thermoneutral, see above. However, the results differ in the case of $V_2O_2^+$. At first glance, our value seems to be more reasonable when calculating the bond dissociation energies for the second oxygen atom, which is anomalously high with the reported figures ($D(V_2O^+ - O) = 7.9$ eV), but lies below 7 eV when our data is used.

As our results are perfectly consistent with the more accurate bond dissociation energies of the monoxides reported in ref 14, we may therefore adopt these values to refine our thermochemical analysis in order to obtain narrower brackets. The figures for the $V_2O_m^+$ species do not change, because the lower limit for $D_0(V_2^+ - O)$ coincides with the reported value. Yet there is a change of about 2 eV for $V_3O_2^+$ and $V_3O_3^+$: $12.1\ \text{eV} \leq D_0(V_3^+ - 2O) \leq 16.2\ \text{eV}$ and $17.3\ \text{eV} \leq D_0(V_3^+ - 3O) \leq 22.7\ \text{eV}$.

Conclusion

Small cationic vanadium clusters are rapidly oxidized. The resulting ions $V_nO_m^+$ continue to easily react with molecular oxygen. In these reactions, degradation of the clusters predominates, which ultimatively yields the mononuclear oxide ions VO^+ and VO_2^+ either directly or after several subsequent steps. Using MS/MS experiments, the interesting details of the complete oxidation of cationic vanadium clusters is explored up to $n = 5$. Moreover, some new thermochemical data for gas-phase vanadium-oxide clusters has been deduced.

Acknowledgment. We thank the Deutsche Forschungsgemeinschaft (SFB 546), the Fonds der Chemischen Industrie, and the Degussa AG for financial support.

References and Notes

(1) (a) Hagen, N. *Technische Katalyse. Eine Einführung*; Wiley-VCH: Weinheim, Germany, 1996. (b) Centi, G.; Cavani, F.; Trifirò, F. *Selective Oxidation by Heterogeneous Catalysis*; Plenum Publishers: New York, 2001.

(2) For a whole issue dedicated to vanadium catalysts, see: Grzybowska-Swierkosz, B.; Trifiro, F. *Appl. Catal. A* **1997**, *157*, 1−2.

(3) (a) Mars, P.; Van Krevelen, D. W. *Chem. Eng. Sci. Spec. Suppl.* **1954**, *3*, 41−59. (b) Rodemerck, U.; Kubias, B.; Zanthoff, H.-W.; Baerns, M. *Appl. Catal. A* **1997**, *153*, 203-216.

(4) Mazurek, U.; Schwarz, H. *Inorg. Chem.* **2000**, *39*, 5586−5590.

(5) (a) Calatayud, M.; Silvi, B.; Andres, J.; Beltran, A. *Chem. Phys. Lett.* **2001**, *333*, 493−503. (b) Calatayud, M.; Andres, J.; Beltran, A. *J. Phys. Chem. A* **2001**, *105*, 9760−9775. (c) Calatayud, M.; Andres, J.; Beltran, A.; Silvi, B. *Theor. Chem. Acc.* **2001**, *105*, 299−308.

(6) (a) Vyboishchikov, S. F.; Sauer, J. *J. Phys. Chem. A* **2000**, *104*, 10913−10922. (b) Vyboishchikov, S. F.; Sauer, J. *J. Phys. Chem. A* **2001**, *105*, 8588−8598.

(7) Johnson, J. R. T.; Panas, I. *Inorg. Chem.* **2000**, *39*, 3192−3204.

(8) Koyanagi, G. K.; Böhme, D. K.; Kretzschmar, I.; Schröder, D.; Schwarz, H. *J. Phys. Chem. A* **2001**, *105*, 4259−4271.

(9) (a) Nieman, G. C.; Parks, E. K.; Richtsmeier, S. C.; Liu, K.; Pobo, L. G.; Riley, S. J. *High Temp. Sci.* **1986**, *22*, 115−138. (b) Rudnyi, E. B.; Kaibicheva, E. A.; Sidorov, L. N. *J. Chem. Thermodyn.* **1993**, *25*, 929−947. (c) Chertihin, G. V.; Bare, W. D.; Andrews, L. *J. Phys. Chem. A* **1997**, *101*, 5090−5096. (d) Bell, R. C.; Zemski, K. A.; Kerns, K. P.; Deng, H. T.; Castleman, A. W. *J. Phys. Chem. A* **1998**, *102*, 1733−1742. (e) Wu, H.; Wang, L.-S. *J. Chem. Phys.* **1998**, *108*, 5310−5318. (f) Foltin, M.; Stueber, G. J.; Bernstein, E. R. *J. Chem. Phys.* **1999**, *111*, 9577−9586. (g) Pramann, A.; Koyasu, K.; Nakajima, A. *J. Chem. Phys.* **2002**, *116*, 6521−6528. (h) Zhai, H.-J.; Wang, L.-S. *J. Chem. Phys.* **2002**, *117*, 7882−7888.

(10) (a) Bell, R. C.; Zemski, K. A.; Castleman, A. W. *J. Phys. Chem. A* **1998**, *102*, 8293−8299. (b) Bell, R. C.; Zemski, K. A.; Castleman, A. W. *J. Phys. Chem. A* **1999**, *103*, 2992−2998. (c) Bell, R. C.; Zemski, K. A.; Castleman, A. W. *J. Phys. Chem. A* **1999**, *103*, 1585−1591. (d) Bell, R. C.; Zemski, K. A.; Castleman, A. W. *J. Cluster. Sci.* **1999**, *10*, 509−524. (f) Bell, R. C.; Zemski, K. A.; Justes, D. R.; Castleman, A. W. *J. Chem. Phys.* **2001**, *114*, 798−811. (g) Zemski, K. A.; Justes, D. R.; Castleman, A. W. *J. Phys. Chem. A* **2001**, *105*, 10237−10245. (h) Zemski, K. A.; Justes, D. R.; Castleman, A. W. *J. Phys. Chem. B* **2002**, *106*, 6136−6148.

(11) Dinca, A.; Davis, T. P.; Fisher, K. J.; Smith, D. R.; Willett, G. D. *Int. J. Mass Spectrom.* **1999**, *182/183*, 73−84.

(12) Asmis, K. R.; Brümmer, M.; Kaposta, C.; Santambrogio, G.; von Helden, G.; Meijer, G.; Rademann, K.; Wöste, L. *Phys. Chem. Chem. Phys.* **2002**, *4*, 1101−1104.

(13) Holmgren, L.; Rosén, A. *J. Chem. Phys.* **1999**, *110*, 2629−2636.

(14) Xu, J.; Rodgers, M. T.; Griffin, J. B.; Armentrout, P. B. *J. Chem. Phys.* **1998**, *108*, 9339−9350.

(15) (a) Eller, K.; Schwarz, H. *Int. J. Mass Spectrom. Ion Processes* **1989**, *93*, 243−257. (b) Eller, K.; Zummack, W.; Schwarz, H. *J. Am. Chem. Soc.* **1990**, *112*, 621−627.

(16) Maruyama, S.; Anderson, L. R.; Smalley, R. E. *Rev. Sci. Instrum.* **1990**, *61*, 3686−3693.

(17) Berg, C.; Schindler, T.; Kantlehner, M.; Niedner-Schatteburg, G.; Bondybey, V. E. *Chem. Phys.* **2000**, *262*, 143−149.

(18) Forbes, R. A.; Laukien, F. H.; Wronka, J. *Int. J. Mass Spectrom. Ion Processes* **1988**, *83*, 23−44.

(19) Wu, H.; Desai, S. R.; Wang, L.-S. *Phys. Rev. Lett.* **1996**, *77*, 2436−2439.

(20) According to a private communication by Prof. P. Armentrout in July 2001, these ions have been detected during their experiments as well but were disregarded in data processing.

(21) Su, T. *J. Chem. Phys.* **1988**, *89*, 5355−5356 and references therein.

(22) (a) Bouchoux, G.; Leblanc, D.; Sablier, M. *Int. J. Mass Spectrom.* **2001**, *210/211*, 189−201. (b) Cooks, R. G.; Patrick, J. S.; Kotiaho, T.; McLuckey, S. A. *Mass Spectrom. Rev.* **1994**, *13*, 287−339.

(23) IE(V) = 6.746 ± 0.002 eV, IE(V_2) = 6.3566 ± 0.0006 eV, according to ref 24.

(24) NIST Standard Reference Database: http://webbook.nist.gov/chemistry.

(25) Harvey, J. N.; Diefenbach, M.; Schröder, D.; Schwarz, H. *Int. J. Mass Spectrom.* **1999**, *182/183*, 85−97.

(26) Figures given without error bars have uncertainties of less than 5 kJ/mol.